International Research Journal of Engineering and Technology (IRJET) e-ISSN: 2395-0056
Volume: 07 Issue: 07 | July 2020 www.irjet.net p-ISSN: 2395-0072

Behavior of NACA 4424, NACA 63(1) - 412 & NACA 63(2) – 615 Airfoils subjected to Subsonic Flow at various Angle of Attacks using CFD

Nagappa Pattanashetti[1], Mahadeva[2], Dr. Suresha C N[3]

[1]*Assistant Professor, Department of Mechanical Engineering, Amruta Institute of Engineering & Management Sciences, Bidadi, Karnataka, India*
[2]*Assistant Professor, Department of Mechanical Engineering, Amruta Institute of Engineering & Management Sciences, Bidadi, Karnataka, India*
[3]*Professor & Head, Department of Mechanical Engineering, Amruta Institute of Engineering & Management Sciences, Bidadi, Karnataka, India*

Abstract – *Aerodynamic behavior of a turbine blade is very important for deciding the performance of a wind turbine. In this study, the aerodynamic performance of three NACA airfoils namely: NACA 4424, NACA 63 (1) – 412 and NACA 63 (2) – 615 have been studied and compared at a subsonic speed for 0, 2, 4, 6, 8 and 10 degrees of angle of attacks using CFD. The aim is to determine the best suitable airfoil to be used for the wing of the turbine depending upon the lift and drag characteristics exhibited by the airfoils. The lift-to-drag ratio has been calculated for all the airfoils and a comparative study is presented. The results show that NACA 63 (2) – 615 exhibits an excellent aerodynamic performance with the highest lift-to-drag ratio for the subsonic speed of study compared to the other two airfoils, except for 4 degrees angle of attack. NACA 4424 exhibits highest drag and lowest lift compared to the other two airfoils. NACA 63 (1) – 412 exhibits an intermediate aerodynamic performance relative to the other two airfoils, but for 4 degrees angle of attack, it exhibits the highest lift-to-drag ratio compared to the other two airfoils.*

Key Words: **Aerofoil, Airfoil, Angle of Attack, CFD, Lift and drag, NACA, Subsonic, Turbine blade.**

1. INTRODUCTION

With the increasing importance of renewable energy, airfoil design, specifically for wind turbines, has become a fundamental issue. Airfoils created for airplanes are occasionally used in wind turbines. In wind turbines the airfoil can be used at a higher angle of attack, sometimes even achieving stall, and the most important parameter is the lift-to-drag ratio [1].

In this regard, various researchers have published their research work by comparative analysis of airfoils using CFD to assess the performance of airfoils. Some of them have been discussed below.

Robiul et. al. conducted a comparative study on different airfoils from NACA and NREL families based on the performance and stability criteria at various Reynold's numbers and angle of attacks. Their study showed that NACA were better performance wise but the NREL airfoils exhibited better stability [2].

Srinivasa et. al. studied the aerodynamic performance of NACA 0012, NACA 4412 and NACA 4418 for different angle of attacks. In their study, it was found that NACA 4412 produced the highest lift. Also, it was found that the drag force of asymmetric airfoil was marginally higher than that of the symmetric airfoil [3].

Despite the present research, due to the large number of airfoils available and also due to the various subsonic flow conditions arising in real-time applications, there is still a large research gap to be closed by analysing the airfoils under these varied flow conditions. Wind tunnel testing can be done to analyse the performance of these airfoils. But the process would be laborious, time-consuming and costly. In contrast, Computational Fluid Dynamics (CFD) provides an easy and cost-effective way to accomplish this big task with fairly accurate results. In this direction, this paper presents a comparative CFD investigation on three airfoils: NACA 4424, NACA 63 (1) – 412 and NACA 63 (2) – 615.

1.1 Airfoil Specifications

The following table details the specifications of the airfoils used in our study.

Table - 1: Specifications of the Airfoils under Study

Name of the Airfoil	Airfoil Specifications		
	Max Thickness	Max Camber	Chord Length
NACA 4424	24% at 29.4% chord	4% at 40% chord	1 metre
NACA 63 (1) - 412	12% at 34.9% chord length	2.2% at 50% chord	1 metre
NACA 63 (2) - 615	15% at 34.8% chord	3.3% at 50% chord	1 metre

2. Methodology

The airfoils were modeled and meshed in 2D using Ansys Gambit 2.4.6 software. The analysis was carried out using Ansys 12 (Fluent) at 0°, 2°, 4°, 8° and 10° angle of attacks. Inlet velocity of 20 m/s was used for the aforementioned angle of attacks (AOA). The coefficient of lift (C_l), coefficient of drag (C_d) were obtained from the analysis and the lift-to-drag ratios were calculated and compared in the analysis.

2.1 Model and Mesh of the Airfoils

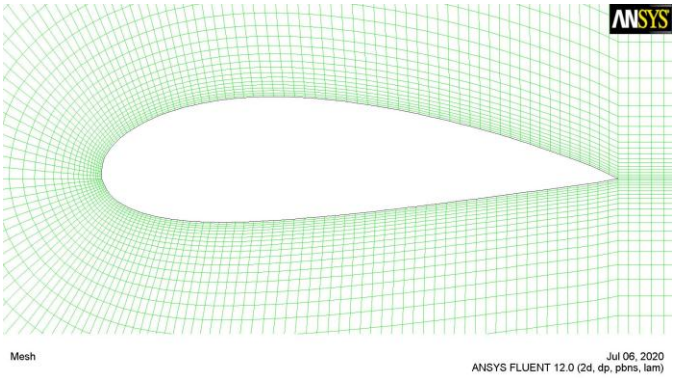

Fig. 1: Meshing of NACA 4424

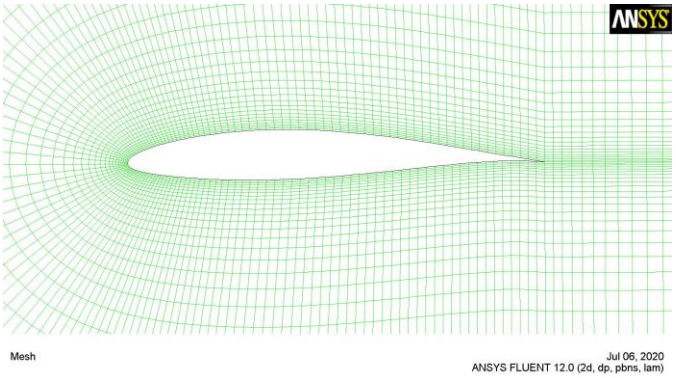

Fig. 2: Meshing of NACA 63(1) – 412

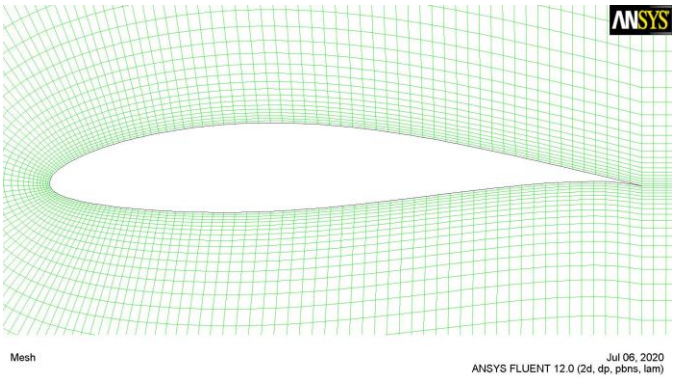

Fig. 3: Meshing of NACA 63(2) – 615

A computational domain of 12.5C has been created around the airfoils for the analysis as shown in the following image.

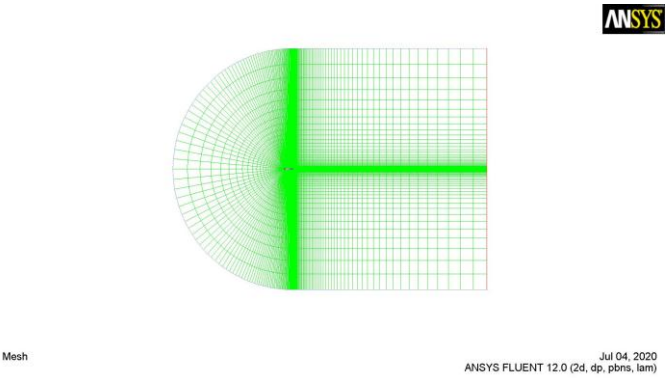

Fig. 4: C-Type Computational Domain for all Airfoils

Table - 2: Details of the Mesh Generated for all the Airfoils

Name of the Airfoil	Details of the Mesh Generated	
	No. of Nodes	No. of Elements
NACA 4424	12465	12060
NACA 63 (1) - 412	12419	12015
NACA 63 (2) - 615	12419	12015

2.2 Operating Conditions and Reynold's Number

The simulations were carried out assuming room temperature conditions at a temperature of 27°Cor 300K. Dry air was selected as the fluid medium and the details of its properties are given in the table below.

Table - 3: Operating Conditions and Dry Air Properties [4]

Operating Temperature	300K
Operating Pressure	101325 Pa
Fluid	Dry Air
Viscosity of air (μ) at 300K	18.46×10^{-6} kg/m-s
Density of air (ρ) at 300K	1.177 kg/m^3
Specific Heat (C_p) at 300K	1.006 kJ/kg-K
Thermal Conductivity (k) at 300K	0.02624 w/m-K

Reynold's number is very important for subsonic flows for fluid velocity ≤ 0.3 Mach, even though it affects airfoils by a small amount [5]. Reynold's Number for an airfoil is given by:

$R_e = VC/\nu$ [5]

Where, R_e =Reynold's Number, C = Chord Length of the Airfoil in metres and ν = Kinematic Viscosity in m^2/s

In our case, V = 20 m/s (≈ 0.0576 Mach), C = 1 m and ν = 15.69×10^{-6} m^2/s (at 300K and atmospheric pressure). Therefore, $R_e = 1.274697 \times 10^6$ ($> 5 \times 10^5$). Hence the flow is

turbulent in nature [5]. We have to choose turbulence model in fluent for our analysis.

2.3 Problem Setup, Boundary Conditions and Solution Method

The details regarding the solver parameters, boundary conditions and solution methods are given in table-4.

Table - 4: Solver Parameters, Boundary Conditions and Solution Methods

Solver Parameters	
Solver Type	Density Based
Time	Steady
Velocity Formulation	Absolute
2D Space	Planar
Multiphase	Off
Energy	On
Viscous Model	Spalart-Allmaras (1 equation)
Spalart-Allmaras Production	Strain/Viscosity-Based
Boundary Conditions	
Inlet Type	Velocity Inlet (20 m/s)
Outlet Type	Pressure Outlet
Wall (No-Slip)	Airfoil
Solution Method	
Pressure Velocity Coupling Scheme	Simple
Gradient	Green-Gauss Node Based
Pressure	Second Order
Momentum	Second Order Upwind
Solution Initialization	From velocity inlet
Convergence Criteria	1×10^{-3}

The lift and the drag forces on the airfoils can be calculated using the following equations [5]:

Lift Force (F_L) = ½ $\rho V^2 A C_l$

Drag Force (F_D) = ½ $\rho V^2 A C_d$

Where, C_l = Coefficient of lift for the airfoil, C_d = Coefficient of drag for the airfoil and A = Planform area of the airfoil = Chord length × Wing span of the airfoil (A = $1m^2$ in our case as the chord length is 1m and the wing span = 1m).

3. Results and Discussion

The coefficients of lift & drag, lift-to-drag ratio and lift & drag forces for the NACA 4424 airfoil at different angle of attacks are presented below in table-5 and table-6.

Table - 5: Coefficients of Lift & Drag and, Lift-to-Drag Ratios for NACA 4424 at various angle of attacks

Angle of Attack (α)	Coefficient of Lift (Cl)	Coefficient of Drag (Cd)	Lift-to-Drag ratio (Cl/Cd)
0	0.252065540	0.017412681	14.475975296
2	0.405795370	0.020482309	19.811993365
4	0.558842530	0.024361980	22.939126048
6	0.691645500	0.030355974	22.784493754
8	0.78799396	0.039689537	19.853946898
10	0.808238610	0.056099785	14.407160562

Table - 6: Lift & Drag Forces for NACA 4424 at various angle of attacks

Angle of Attack (α)	Lift Force (N)	Drag Force (N)
0	59.33622812	4.09894511
2	95.5242301	4.82153554
4	131.5515316	5.73481009
6	162.8133507	7.14579628
8	185.4937782	9.34291701
10	190.2593688	13.2058894

It is observed from table-5 for NACA 4424, that the peak lift-to-drag ratio is achieved at 4° angle of attack. At 6° angle of attack, the lift-to-drag ratio decreases even though the lift force is increasing. To understand this, we can refer the contours of static pressure and velocity magnitude given in figure 5 to 8 below.

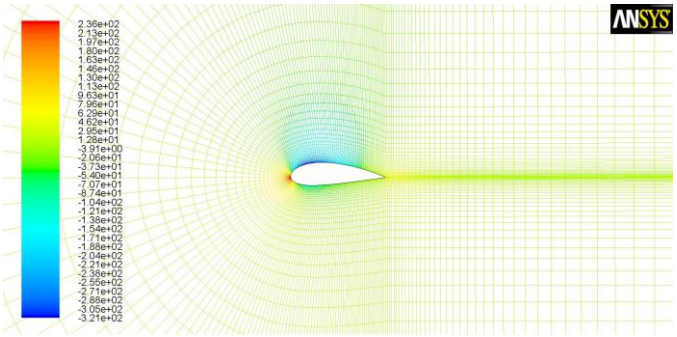

Fig. 5: Contours of Static Pressure for 4° AOA – NACA 4424

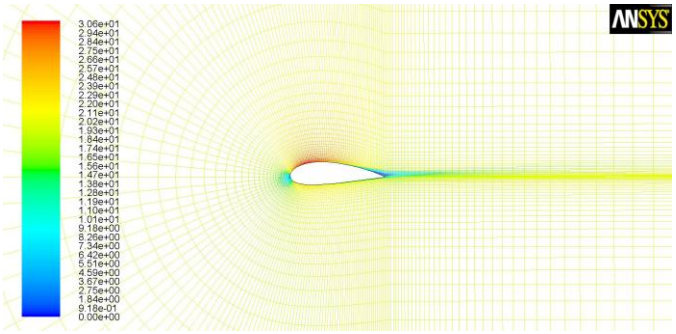

Fig. 6: Contours of Velocity Magnitude for 4° AOA – NACA 4424

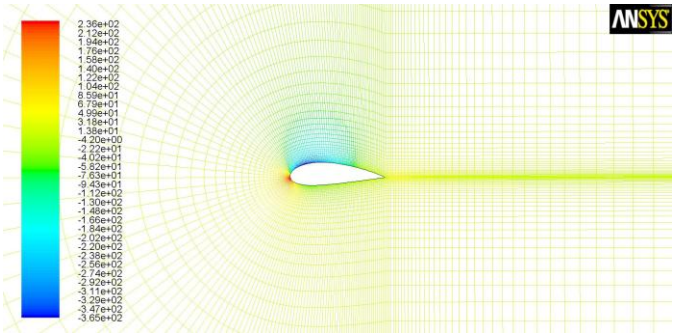

Fig. 7: Contours of Static Pressure for 6° AOA – NACA 4424

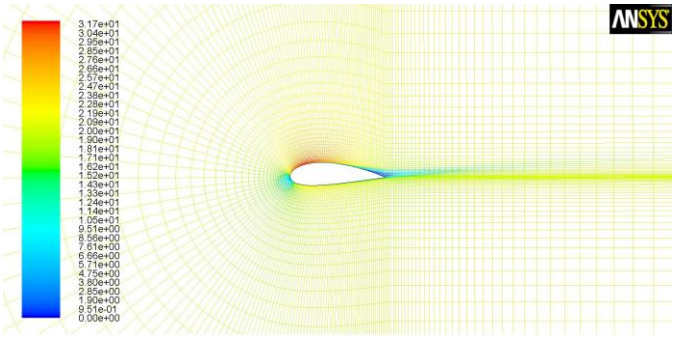

Fig. 8: Contours of Velocity Magnitude for 6° AOA – NACA 4424

It can be observed from the contours of static pressure that the stagnation point is located near the leading edges for both the cases. Because of the higher static pressure below the airfoil, the airfoil experiences lift in both the cases. Also, on comparing the contours of velocity magnitude, it can be seen that lower air velocity magnitude occurs on the upper surface of the airfoil near the trailing edge. This indicates a higher static pressure in that region for both the cases according to Bernoulli's principle. This higher static pressure induces drag in the airfoil. The drag is higher for the 6° angle of attack case when compared to the 4° angle of attack case. This is because the velocity contour is more prominent near the trailing edge in case of 6° angle of attack case, leading to a higher static pressure, hence higher drag. Thus, the overall lift-to-drag ratio decreases for 6° angle of attack case even though the lift is increasing. For subsequent angle of attacks, the drag induced increases and hence, the lift-to-drag ratio keeps decreasing.

The coefficients of lift & drag, lift-to-drag ratio and lift & drag forces for the NACA 63(1) - 412 airfoil at different angle of attacks are presented below in table-7 and table-8.

Table - 7: Coefficients of Lift & Drag and, Lift-to-Drag Ratios for NACA 63 (1) – 412 at various angle of attacks

Angle of Attack (α)	Coefficient of Lift (Cl)	Coefficient of Drag (Cd)	Lift-to-Drag ratio (Cl/Cd)
0	0.32154256	0.01136149	28.30110324
2	0.538760810	0.012001150	44.89243198
4	0.737413900	0.014521995	50.77910439
6	0.930130930	0.020642446	45.05914318
8	1.092623300	0.027794439	39.31085999
10	1.167495800	0.044378226	26.30785196

Table - 8: Lift & Drag Forces for NACA 63(1) - 412 at various angle of attacks

Angle of Attack (α)	**Lift Force (N)**	**Drag Force (N)**
0	75.69111862	2.67449357
2	126.8242947	2.82507071
4	173.5872321	3.41847762
6	218.9528209	4.85923179
8	257.2035248	6.54281094
10	274.8285113	10.4466344

It is observed from table-7 for NACA 63(1) - 412, that the peak lift-to-drag ratio is achieved at 4° angle of attack. At 6° angle of attack, the lift-to-drag ratio decreases even though the lift force is increasing. To understand this, we can refer the contours of static pressure and velocity magnitude given in figure 9 to 12 below.

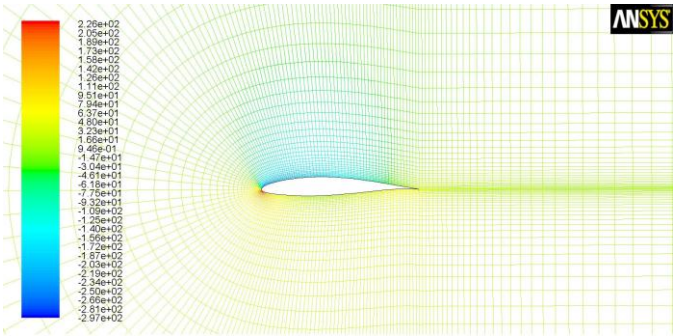

Fig. 9: Contours of Static Pressure for 4° AOA – NACA 63(1) – 412

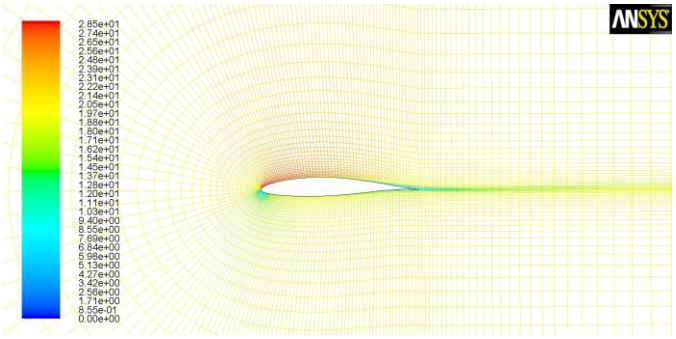

Fig. 10: Contours of Velocity Magnitude for 4° AOA – NACA 63(1) – 412

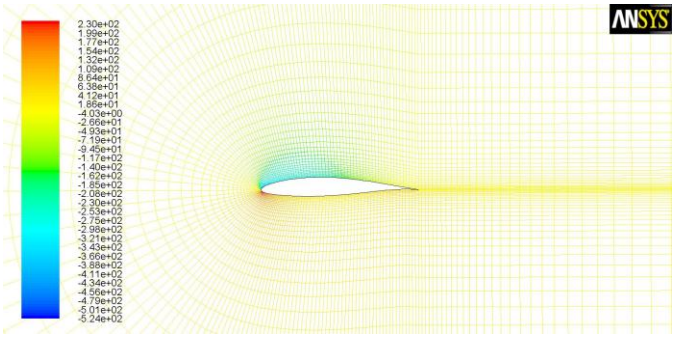

Fig. 11: Contours of Static Pressure for 6° AOA – NACA 63(1) – 412

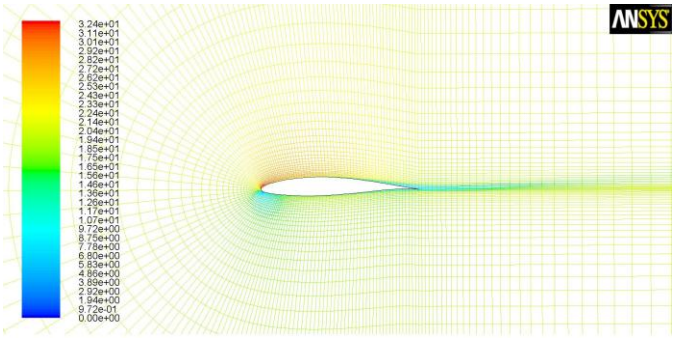

Fig. 12: Contours of Velocity Magnitude for 6° AOA – NACA 63(1) – 412

It can be observed from the contours of the static pressure that the stagnation point exists near the leading edge of the airfoil in both the cases. Because of the higher static pressure below the airfoil, the airfoil experiences lift in both the cases. On comparing the contours of velocity magnitude for both the cases, it clear that a low air velocity magnitude exists on the upper surface of the airfoil near the trailing edge. Hence a higher static pressure occurs there according to Bernoulli's principle, causing a drag in the airfoil. It can be seen that this low velocity contour is more prominent in the 6° angle of attack case, indicating a higher static pressure and hence, higher drag. Thus, even though the lift increases for the 6° angle of attack case, the lift-to-drag ratio still decreases because of the increased drag compared to the 4° case. For subsequent angle of attacks, the drag induced increases and hence, the lift-to-drag ratio keeps decreasing.

The coefficients of lift & drag, lift-to-drag ratio and lift & drag forces for the NACA 63(2) - 615 airfoil at different angle of attacks are presented below in table-9 and table-10.

Table - 9: Coefficients of Lift & Drag and, Lift-to-Drag Ratios for NACA 63 (2) – 615 at various angle of attacks

Angle of Attack (α)	Coefficient of Lift (Cl)	Coefficient of Drag (Cd)	Lift-to-Drag ratio (Cl/Cd)
0	0.48431622	0.01298162	37.30782990
2	0.695491280	0.014830532	46.89590906
4	0.891060840	0.018564710	47.99756312
6	1.070936500	0.022074091	48.51554250
8	1.264088600	0.027732157	45.58205119
10	1.355183200	0.038670715	35.04417231

Table - 10: Lift & Drag Forces for NACA 63(2) - 615 at various angle of attacks

Angle of Attack (α)	**Lift Force (N)**	**Drag Force (N)**
0	114.0080382	3.05587429
2	163.7186473	3.49110723
4	209.7557217	4.37013273
6	252.0984521	5.19624102
8	297.5664564	6.52814976
10	319.0101253	9.10308631

It is observed from table-9 for NACA 63(2) - 615, that the peak lift-to-drag ratio is achieved at 6° angle of attack. At 8° angle of attack, the lift-to-drag ratio decreases even though the lift force is increasing. To understand this, we can refer the contours of static pressure and velocity magnitude given in figure 13 to 16 below.

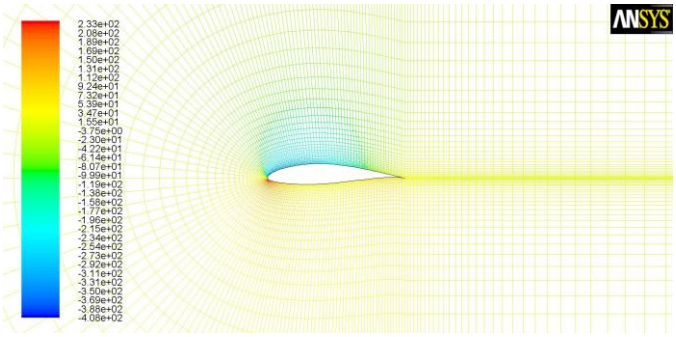

Fig. 13: Contours of Static Pressure for 6° AOA – NACA 63(2) – 615

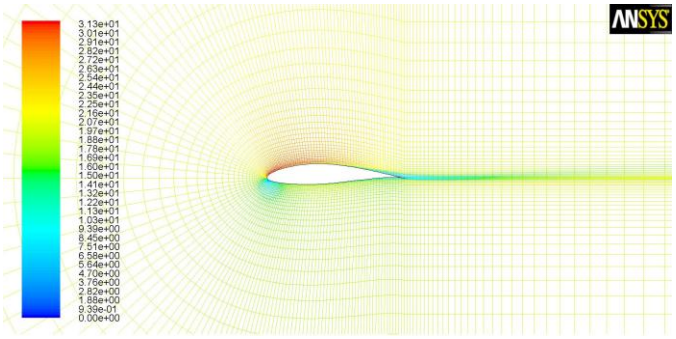

Fig. 14: Contours of Velocity Magnitude for 6° AOA – NACA 63(2) – 615

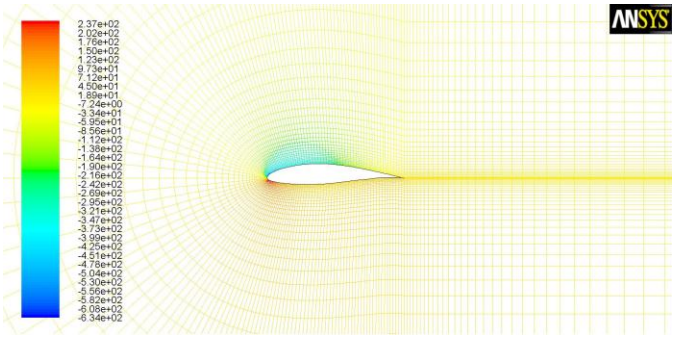

Fig. 15: Contours of Static Pressure for 8° AOA – NACA 63(2) – 615

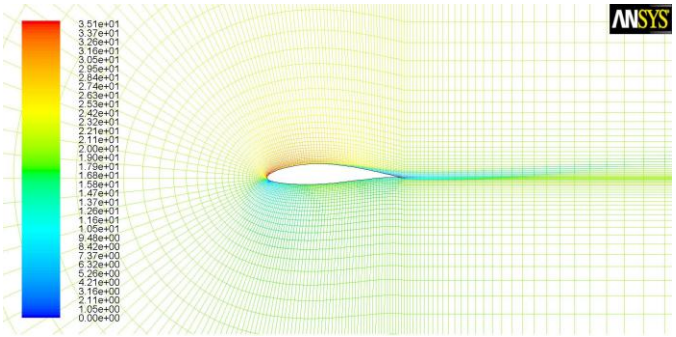

Fig. 16: Contours of Velocity Magnitude for 8° AOA – NACA 63(2) – 615

It can be observed from the contours of the static pressure that the stagnation point exists slightly below the leading edge of the airfoil in both the cases. Because of the higher static pressure below the airfoil, the airfoil experiences lift in both the cases. On comparing the contours of velocity magnitude for both the cases, it is clear that a low air velocity magnitude exists on the upper surface of the airfoil near the trailing edge. Hence a higher static pressure occurs there according to Bernoulli's principle, causing a drag in the airfoil. It can be seen that this low velocity contour is more prominent in the 8° angle of attack case, indicating a higher static pressure and hence, higher drag. Thus, even though the lift increases for the 8° angle of attack case, the lift-to-drag ratio still decreases because of the increased drag compared to the 6° case. For subsequent angle of attacks, the drag induced increases and hence, the lift-to-drag ratio keeps decreasing.

The following charts give a comparison between the lift and drag characteristics of all the airfoils under our study.

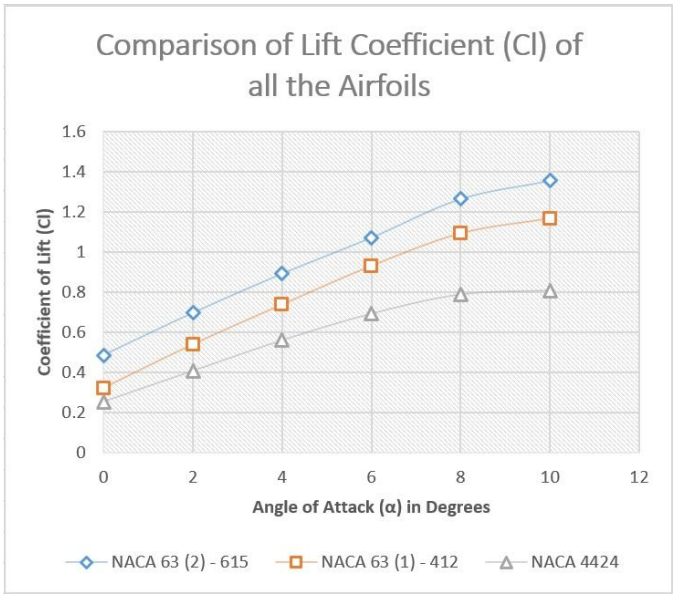

Chart – 1: Comparison of Lift Coefficients for all the Airfoils

It is observed from chart – 1 that NACA 63 (2) – 615 exhibits the highest lift compared to the other two airfoils. NACA 63 (1) – 412 exhibits intermediate lift characteristics and NACA 4424 exhibits the lowest lift characteristics.

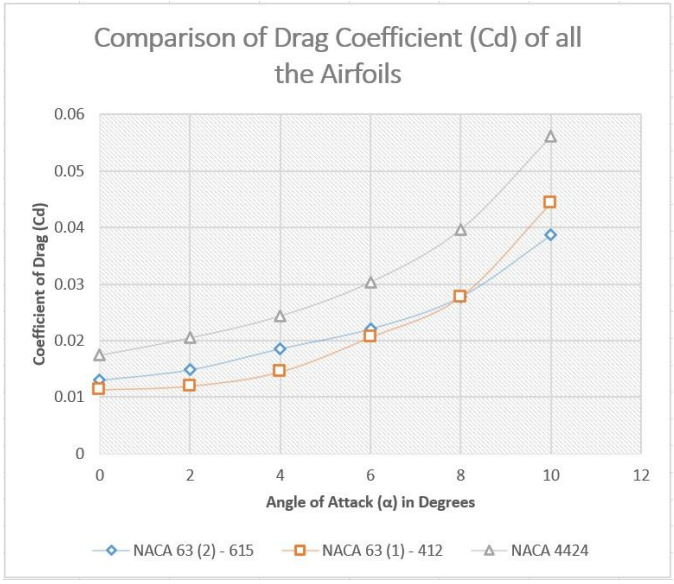

Chart – 2: Comparison of Drag Coefficients for all the Airfoils

It is observed from chart – 2 that NACA 4424 exhibits the highest drag compared to the other two airfoils, with NACA 63(1) – 412 exhibiting the least drag up to 8° angle of attack. At 10° angle of attack, NACA 63(1) – 412 exhibits a higher drag compared to NACA 63 (2) – 615, which exhibits the lowest drag amongst all at 10° angle of attack.

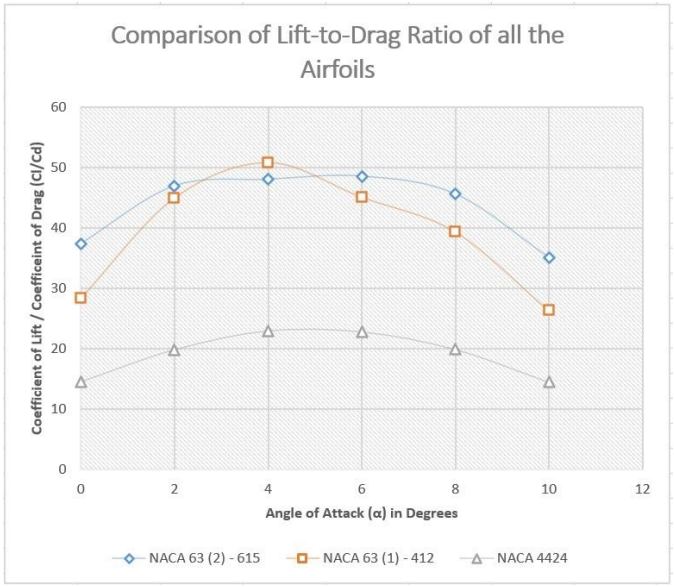

Chart – 3: Comparison of Lift-to-Drag ratio for all the Airfoils

It is observed from chart -3 that NACA 63(2) – 615 exhibits the highest lift-to-drag ratio compared to the other two airfoils, except for the 4° angle of attack case. For 4° angle of attack, NACA 63(1) – 412 exhibits the highest lift-to-drag ratio. NACA 4424 exhibits the lowest lift-to-drag ratio out of all the airfoils for all the angle of attacks.

4. CONCLUSIONS

For any turbine blade, the lift-to-drag ratio it exhibits is the most important factor that directly affects the efficiency of the turbine. For the same reason, some of the airfoils are used in turbines even beyond their stall angle, unlike aerospace applications, where a stall is considered as a limitation and the performance criteria is different.

In our study, based on the results obtained by comparing the aerodynamic performance of NACA 4424, NACA 63(1) – 412 and NACA 63(2) – 615, it can be concluded that the NACA 63(1) – 412 and NACA 63(2) – 615 clearly outperform NACA 4424 in all the aspects. For all the angle of attacks (except for 4° angle of attack), the NACA 63(2) – 615 can be chosen over the other two airfoils for the wind turbine blade design. But for a typical wind turbine design with 4° angle of attack, NACA 63(1) – 412 can be chosen over the other two airfoils as it exhibits the highest lift-to-drag ratio.

REFERENCES

[1] A.F.P. Ribeiro, A.M. Awruch, H.M. Gomes, "An airfoil optimization technique for wind turbines", Pg. 4898-4907, doi:10.1016/j.apm.2011.12.026.

[2] Md. Robiul Islam, Labid Bin Bashar, Dip Kumar Saha, NazmusSowad Rafi, "Comparison and Selection of Airfoils for Small Wind Turbine between NACA and NREL's S series Airfoil Families", Pg. 1-11, doi: http://doi.org/10.5281/zenodo.3520469.

[3] K Srinivasa Rao, M Ashok Chakravarthy, G Sreedhara Babu, M Rajesh, "Modeling and Simulation of Aerofoil Element", International Research Journal of Engineering and Technology (IRJET), Pg. 2056-2059, Volume 05, Issue 02, Feb 2018, e-ISSN: 2395-0056, p-ISSN: 2395-0072.

[4] Richard W. Johnson, "Handbook of Fluid Dynamics", Second Edition, Appendix C, C-2, Table C.1, CRS Press, Taylor & Francis Group, ISBN-13: 978-1-4398-4957-6.

[5] Frank M. White, "Fluid Mechanics", Seventh Edition, Pg. No. 498, 484, 474 and 501, McGraw Hill Publications, ISBN: 978-0-07-352934-9.

BIOGRAPHIES

"Nagappa Pattanashetti has four years of teaching experience. His research area of interest are Fluid Mechanics and Friction Stir Welding. He has published one paper in international journal and has presented three papers in national conferences".

"Mahadeva has seven years of industrial experience and four years of teaching experience. His research area of interest is Thermal Power Engineering and Biofuels. He has published four papers in national journals and two papers in international journals. He has presented several papers in national and international conferences".

"Dr. Suresha C N has thirty years of teaching experience. His research area of interest is Friction Stir Welding. He has published several papers in national & international journals. He has also presented several papers in national and international conferences. He is presently guiding two PhD. research scholars under Visvesvaraya Technological University, Belagavi, Karnataka, India".